Electronic Supplementary Material (ESI) for Dalton Transactions.

Novel mononuclear Ln complexes with pyrazine-2-carboxylate and acetylacetonate co-ligands: remarkable Single Molecule Magnet behavior of Yb derivative

Andrey V. Gavrikov [a], Nikolay N. Efimov [a,*], Zhanna V. Dobrokhotova [a], Andrey B. Ilyukhin [a], Pavel N. Vasilyev, Vladimir M. Novotortsev [a]

[a] *N.S. Kurnakov Institute of General and Inorganic Chemistry, Russian Academy of Sciences, Leninsky prosp. 31, 119991 Moscow, Russian Federation. E-mail: nnefimov@yandex.ru*

Contents

Table S1. Crystal data and structure refinement for **1-9**.

Identification code	**1**	**2**	**3**	**4**
Empirical formula	$C_{15}H_{21}EuN_2O_8$	$C_{15}H_{21}GdN_2O_8$	$C_{15}H_{21}N_2O_8Tb$	$C_{15}H_{21}DyN_2O_8$
Formula weight	509.30	514.59	516.26	519.84
Temperature, K	173(2)	173(2)	150(2)	173(2)
Wavelength, Å	0.71073	0.71073	0.71073	0.71073
Crystal system	Monoclinic	Monoclinic	Monoclinic	Monoclinic
Space group	$P2_1/n$	$P2_1/n$	$P2_1/n$	$P2_1/n$
a, Å	7.8334(9)	7.8191(9)	7.7951(5)	7.7900(5)
b, Å	30.012(4)	29.984(3)	29.903(2)	29.8733(18)
c, Å	8.2681(10)	8.2673(9)	8.2627(6)	8.2641(5)
β, °	106.095(2)	105.950(2)	105.8510(10)	105.941(2)
Volume, $Å^3$	1867.6(4)	1863.6(3)	1852.8(2)	1849.2(2)
Z	4	4	4	4
D (calc), Mg/m^3	1.811	1.834	1.851	1.867
μ, mm^{-1}	3.402	3.603	3.861	4.085
F(000)	1008	1012	1016	1020
Crystal size, mm	0.34 x 0.26 x 0.1	0.1 x 0.1 x 0.06	0.4 x 0.32 x 0.2	0.32 x 0.28 x 0.1
θ range, °	2.652, 31.556	2.651, 30.606	2.651, 31.564	2.652, 28.281
Index ranges	-11<=h<=11 -42<=k<=44 -12<=l<=12	-11<=h<=7 -42<=k<=42 -11<=l<=11	-11<=h<=11 -43<=k<=43 -12<=l<=11	-10<=h<=10 -39<=k<=39 -11<=l<=11
Reflections collected	23238	16029	21133	22347
Independent reflections, Rint	6097, 0.0404	5575, 0.0375	6036, 0.0359	4583, 0.0872
Completeness to θ = 25.242°	100.0 %	99.5 %	100.0 %	100.0 %
Absorption correction	Semi-empirical from equivalents	Semi-empirical from equivalents	Semi-empirical from equivalents	Semi-empirical from equivalents
Max,. min. transmission	0.7462, 0.5651	0.7461, 0.65	0.7462, 0.5086	0.7465, 0.4472
Refinement method	Full-matrix least-squares on F^2	Full-matrix least-squares on F^2	Full-matrix least-squares on F^2	Full-matrix least-squares on F^2
Data / restraints / parameters	6097 / 0 / 239	5575 / 0 / 239	6036 / 0 / 239	4583 / 0 / 239
Goodness-of-fit	1.168	1.105	1.136	1.222
R1, wR2 [I>2sigma(I)]	0.0394, 0.0803	0.0411, 0.0761	0.0335, 0.0652	0.0434, 0.1100
R1, wR2 (all data)	0.0472, 0.0830	0.0562, 0.0804	0.0396, 0.0671	0.0462, 0.1114
Largest diff. peak and hole, $e.Å^{-3}$	1.260, -2.056	1.257, -2.339	1.028, -1.348	1.496, -2.223

Identification code	**5**	**6**	**7**	**8**	**9**
Empirical formula	$C_{15}H_{21}HoN_2O_8$	$C_{15}H_{21}ErN_2O_8$	$C_{15}H_{21}N_2O_8Tm$	$C_{15}H_{21}N_2O_8Yb$	$C_{15}H_{21}N_2O_8Y$
Formula weight	522.27	524.60	526.27	530.38	446.25
Temperature, K	150(2)	150(2)	150(2)	150(2)	120(2)
Wavelength, Å	0.71073	0.71073	0.71073	0.71073	0.71073
Crystal system	Monoclinic	Monoclinic	Monoclinic	Monoclinic	Monoclinic
Space group	$P2_1/n$	$P2_1/n$	$P2_1/n$	$P2_1/n$	$P2_1/n$
a, Å	7.7665(4)	7.7499(8)	7.7410(7)	7.7360(7)	7.7630(5)
b, Å	29.8018(15)	29.727(3)	29.734(3)	29.710(2)	29.772(2)
c, Å	8.2632(4)	8.2564(9)	8.2614(7)	8.2611(7)	8.2595(6)
β, °	105.8680(10)	105.8480(10)	105.8110(10)	105.765(2)	105.8460(10)
Volume, $Å^3$	1839.68(16)	1829.8(3)	1829.6(3)	1827.3(3)	1836.4(2)
Z	4	4	4	4	4
D (calc), Mg/m^3	1.886	1.904	1.911	1.928	1.614
μ, mm^{-1}	4.345	4.631	4.894	5.163	3.220
F(000)	1024	1028	1032	1036	912
Crystal size, mm	0.3 x 0.24 x 0.1	0.3 x 0.22 x 0.12	0.32 x 0.24 x 0.1	0.24 x 0.2 x 0.1	0.28 x 0.16 x 0.1
θ range, °	2.652, 31.064	2.654, 25.848	2.652, 31.530	2.652, 31.101	2.653, 31.005
Index ranges	-11<=h<=11 -43<=k<=42 -11<=l<=11	-9<=h<=9 -36<=k<=36 -10<=l<=10	-11<=h<=11 -43<=k<=43 -11<=l<=12	-11<=h<=10 -42<=k<=42 -11<=l<=11	-11<=h<=11 -42<=k<=41 -11<=l<=11
Reflections collected	22854	13406	20052	18741	22694
Independent reflections, Rint	5845, 0.0329	3527, 0.0928	5941, 0.0484	5726, 0.0487	5789, 0.0528
Completeness to θ = 25.242°	100.0 %	99.8 %	100.0 %	99.9 %	100.0 %
Absorption correction	Semi-empirical from equivalents	Semi-empirical from equivalents	Semi-empirical from equivalents	Semi-empirical from equivalents	Semi-empirical from equivalents
Max,. min. transmission	0.7462, 0.5243	0.7462, 0.4999	0.7462, 0.4999	0.7462, 0.5435	0.648, 0.3597
Refinement method	Full-matrix least-squares on F^2	Full-matrix least-squares on F^2	Full-matrix least-squares on F^2	Full-matrix least-squares on F^2	Full-matrix least-squares on F^2
Data / restraints / parameters	5845 / 0 / 239	3527 / 6 / 239	5941 / 0 / 239	5726 / 0 / 239	5789 / 0 / 239
Goodness-of-fit	1.562	1.607	1.077	1.009	1.052
R1, wR2 [I>2sigma(I)]	0.0390, 0.0721	0.0450, 0.0864	0.0377, 0.0765	0.0371, 0.0785	0.0385, 0.0815
R1, wR2 (all data)	0.0425, 0.0728	0.0479, 0.0872	0.0508, 0.0807	0.0507, 0.0836	0.0584, 0.0870
Largest diff. peak and hole, $e.Å^{-3}$	1.760, -1.881	1.465, -2.600	1.241, -1.530	1.207, -1.290	0.727, -0.495

Table S2. Bond lengths [Å] for **1-9**.

	Eu	Gd	Tb	Dy	Ho	Er	Tm	Yb	Y
Ln(1)-O(1)	2.340(2)	2.333(3)	2.322(2)	2.303(4)	2.302(3)	2.289(4)	2.280(3)	2.270(3)	2.3012(15)
Ln(1)-O(2)	2.314(2)	2.302(3)	2.290(2)	2.275(4)	2.270(3)	2.261(4)	2.246(3)	2.239(3)	2.2683(15)
Ln(1)-O(3)	2.319(3)	2.310(3)	2.295(2)	2.290(4)	2.274(3)	2.261(5)	2.255(3)	2.255(3)	2.2752(16)
Ln(1)-O(4)	2.350(3)	2.343(3)	2.332(2)	2.317(4)	2.311(3)	2.296(4)	2.289(3)	2.279(3)	2.3107(15)
Ln(1)-O(5)	2.416(2)	2.411(3)	2.391(2)	2.376(4)	2.364(3)	2.352(4)	2.344(3)	2.328(3)	2.3657(15)
Ln(1)-O(7)	2.479(2)	2.465(3)	2.446(2)	2.435(4)	2.421(3)	2.408(4)	2.397(3)	2.385(3)	2.4175(15)
Ln(1)-O(8)	2.485(2)	2.472(3)	2.460(2)	2.445(4)	2.427(3)	2.411(4)	2.406(3)	2.399(3)	2.4236(15)
Ln(1)-N(1)	2.640(3)	2.620(3)	2.609(2)	2.590(4)	2.577(3)	2.557(4)	2.561(3)	2.550(3)	2.5874(17)

Table S3. Hydrogen bonds for **1-9** [Å and °].

D-H...A	d(D-H)	d(H...A)	d(D...A)	<(DHA)
		Eu		
O(7)-H(1)...O(6)#1	0.83	1.91	2.705(3)	161
O(7)-H(2)...N(2)#2	0.88	1.98	2.836(4)	164
O(8)-H(4)...O(6)#3	0.73	2.22	2.846(3)	144
O(8)-H(3)...O(6)#1	0.88	1.89	2.747(3)	164
C(13)-H(13A)...O(5)#4	0.95	2.49	3.403(4)	161
C(14)-H(14A)...O(1)	0.95	2.56	3.097(4)	116
		Gd		
O(7)-H(1)...O(6)#1	0.92	1.79	2.706(4)	174
O(7)-H(2)...N(2)#2	0.91	1.93	2.841(4)	174
O(8)-H(3)...O(6)#3	0.94	1.98	2.848(4)	153
O(8)-H(4)...O(6)#1	0.77	1.98	2.744(4)	176
C(13)-H(13A)...O(5)#4	0.95	2.48	3.398(5)	162
C(14)-H(14A)...O(1)	0.95	2.56	3.091(5)	116
		Tb		
O(7)-H(1)...O(6)#1	0.82	1.90	2.701(3)	165
O(7)-H(2)...N(2)#2	0.77	2.07	2.841(3)	174
O(8)-H(3)...O(6)#3	0.83	2.13	2.853(3)	146
O(8)-H(4)...O(6)#1	0.84	1.92	2.747(3)	169
C(13)-H(13A)...O(5)#4	0.95	2.48	3.393(4)	162
C(14)-H(14A)...O(1)	0.95	2.54	3.073(4)	116
		Dy		
O(7)-H(1)...O(6)#1	0.75	1.97	2.707(5)	172
O(7)-H(2)...N(2)#2	0.86	2.00	2.846(6)	167
O(8)-H(4)...O(6)#3	0.89	2.04	2.859(5)	153
O(8)-H(3)...O(6)#1	0.78	2.04	2.745(5)	152
C(13)-H(13A)...O(5)#4	0.95	2.49	3.401(7)	162
C(14)-H(14A)...O(1)	0.95	2.55	3.069(7)	115
		Ho		
O(7)-H(1)...O(6)#1	0.80	1.91	2.702(4)	171
O(7)-H(2)...N(2)#2	0.82	2.05	2.844(4)	163
O(8)-H(3)...O(6)#1	0.82	1.95	2.744(4)	163
O(8)-H(4)...O(6)#3	0.81	2.11	2.855(4)	154

C(13)-H(13A)...O(5)#4	0.95	2.49	3.404(4)	162
C(14)-H(14A)...O(1)	0.95	2.53	3.048(5)	114
		Er		
O(7)-H(1)...O(6)#1	0.90	1.84	2.700(5)	158
O(7)-H(2)...N(2)#2	0.79	2.08	2.842(6)	162
O(8)-H(3)...O(6)#3	0.90	2.00	2.852(5)	158
O(8)-H(4)...O(6)#1	0.78	1.99	2.738(6)	162
C(13)-H(13A)...O(5)#4	0.95	2.49	3.405(6)	162
C(14)-H(14A)...O(1)	0.95	2.53	3.035(7)	114
		Tm		
O(7)-H(1)...N(2)#2	0.82	2.10	2.843(4)	150
O(7)-H(2)...O(6)#1	0.82	1.92	2.695(4)	160
O(8)-H(3)...O(6)#1	0.80	1.98	2.748(4)	160
O(8)-H(4)...O(6)#3	0.86	2.10	2.860(4)	148
C(13)-H(13A)...O(5)#4	0.95	2.49	3.408(5)	163
C(14)-H(14A)...O(1)	0.95	2.52	3.033(5)	114
		Yb		
O(7)-H(1)...N(2)#2	0.90	1.97	2.852(4)	168
O(7)-H(2)...O(6)#1	0.86	1.88	2.697(4)	160
O(8)-H(3)...O(6)#3	0.92	1.98	2.873(4)	162
O(8)-H(4)...O(6)#1	0.88	1.94	2.753(4)	153
C(13)-H(13A)...O(5)#4	0.95	2.49	3.408(4)	163
C(14)-H(14A)...O(1)	0.95	2.52	3.028(5)	113
		Y		
O(7)-H(2)...N(2)#2	0.91	1.94	2.837(2)	168
O(7)-H(1)...O(6)#1	0.82	1.90	2.696(2)	164
O(8)-H(4)...O(6)#1	0.78	2.02	2.745(2)	155
O(8)-H(3)...O(6)#3	0.85	2.05	2.854(2)	157
C(13)-H(13A)...O(5)#4	0.95	2.48	3.396(3)	162
C(14)-H(14A)...O(1)	0.95	2.54	3.053(3)	114

Symmetry transformations used to generate equivalent atoms:

#1 -x, -y, -z; #2 -x, -y, -z+1; #3 x+1, y, z; #4 x, y, z+1

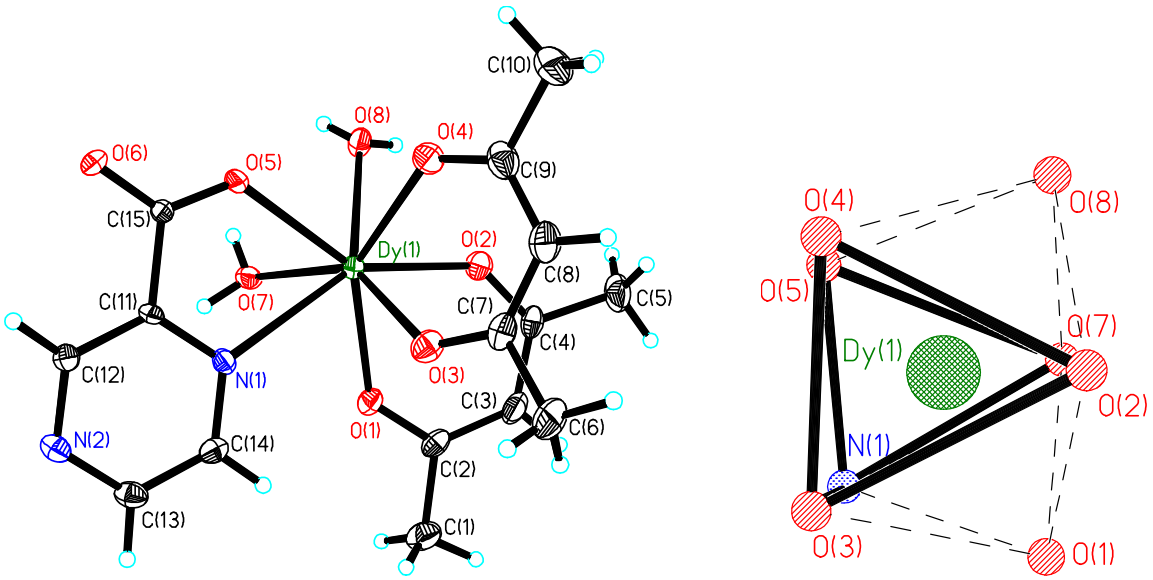

a **b**

Fig.S1. Molecular structure of complex **4**, $[Dy(acac)_2(PyrCOO)(H_2O)_2]$ (**a**), and coordination environment of Dy atom (**b**).

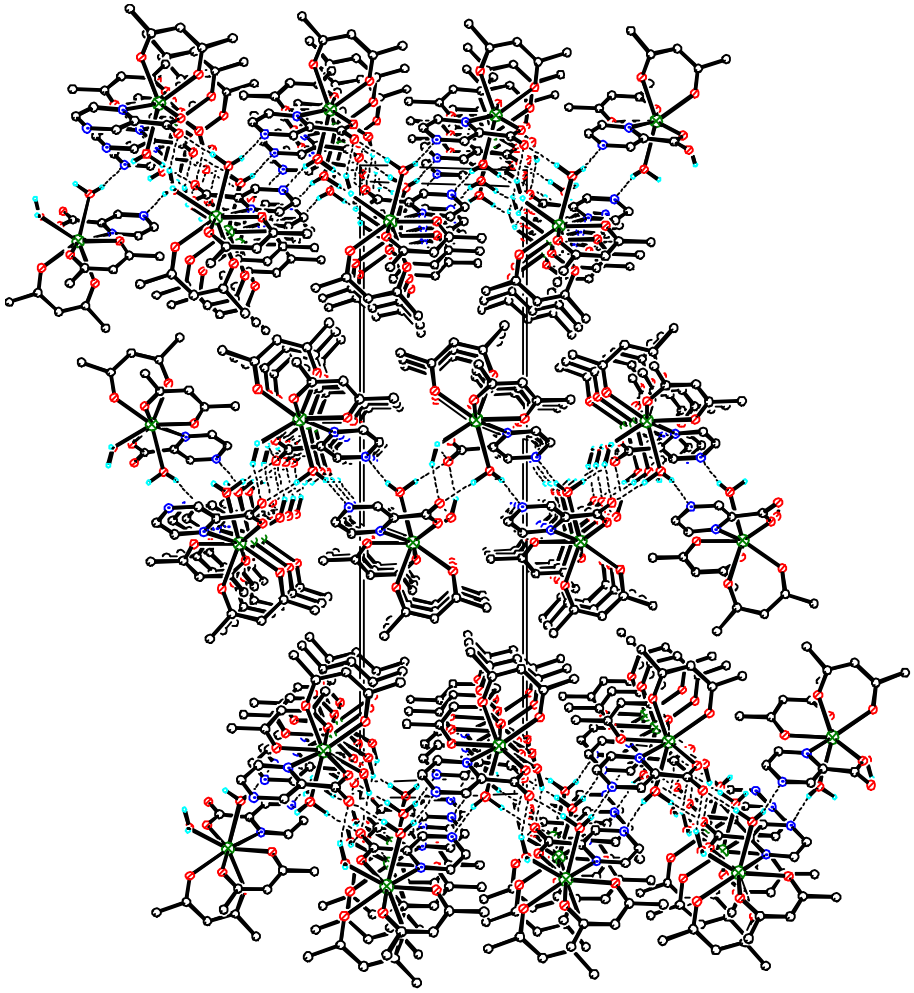

a

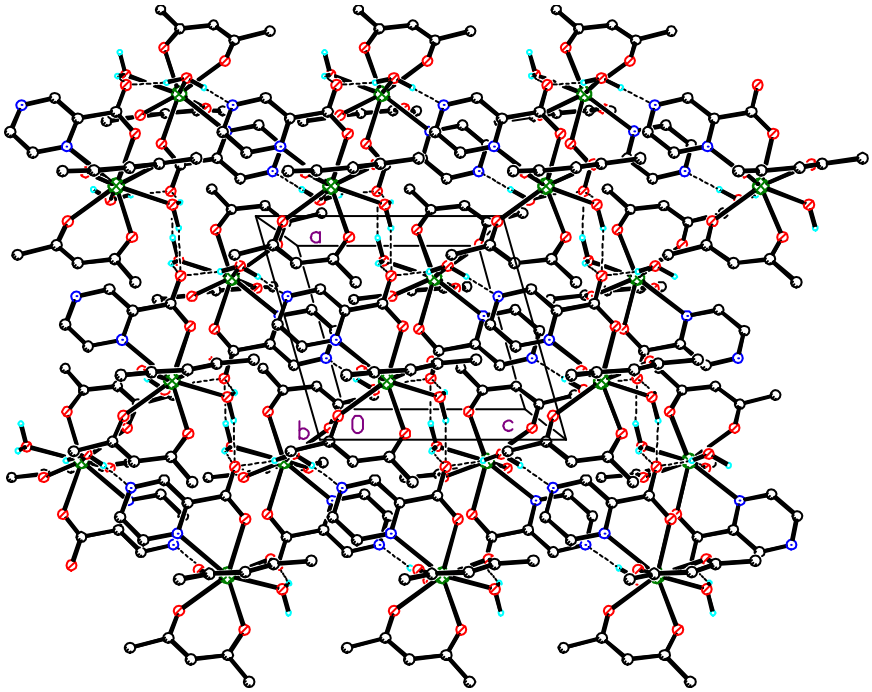

b

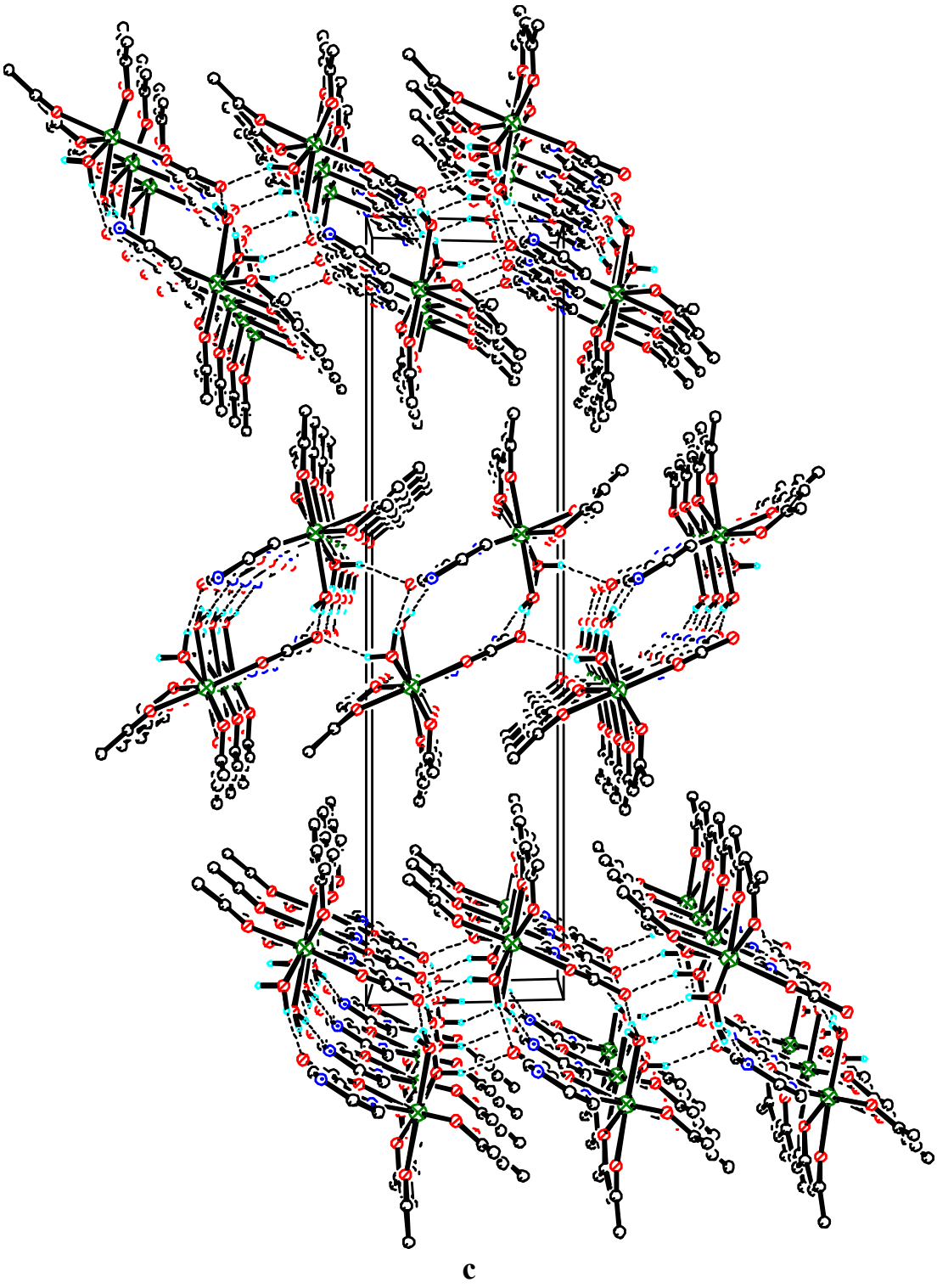

Fig.S2. Projection of structure **4** (Dy) along the axis: *x* (a); *y*, one layer is shown, (b); *z* (c).

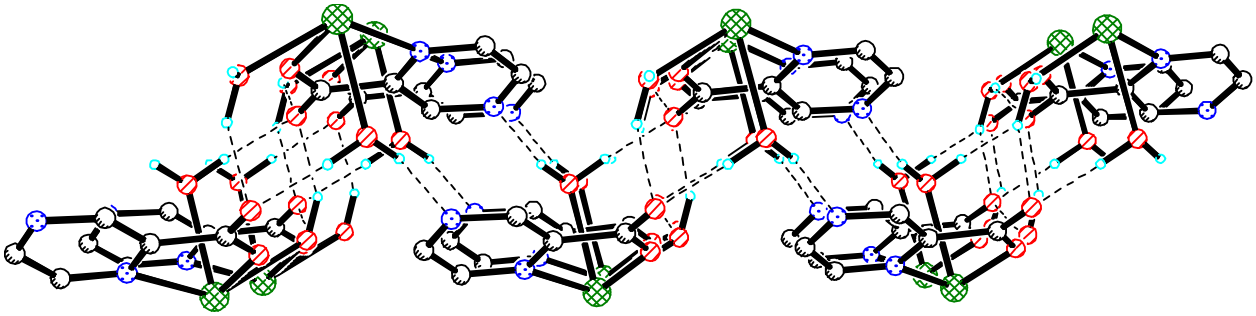

a

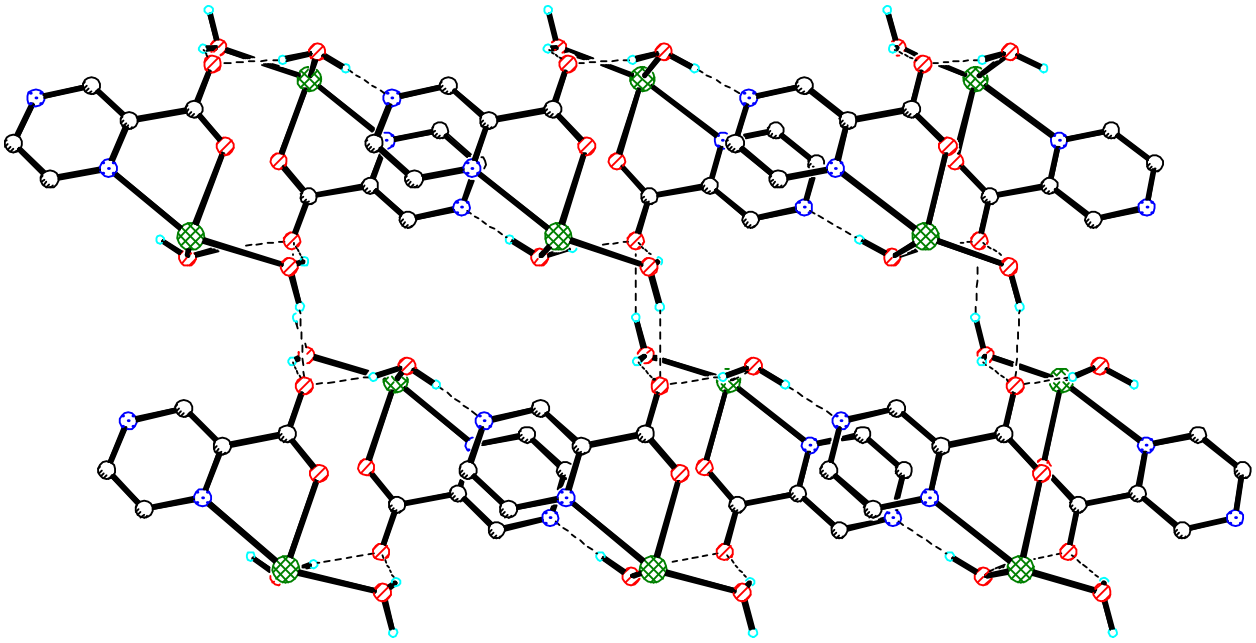

b

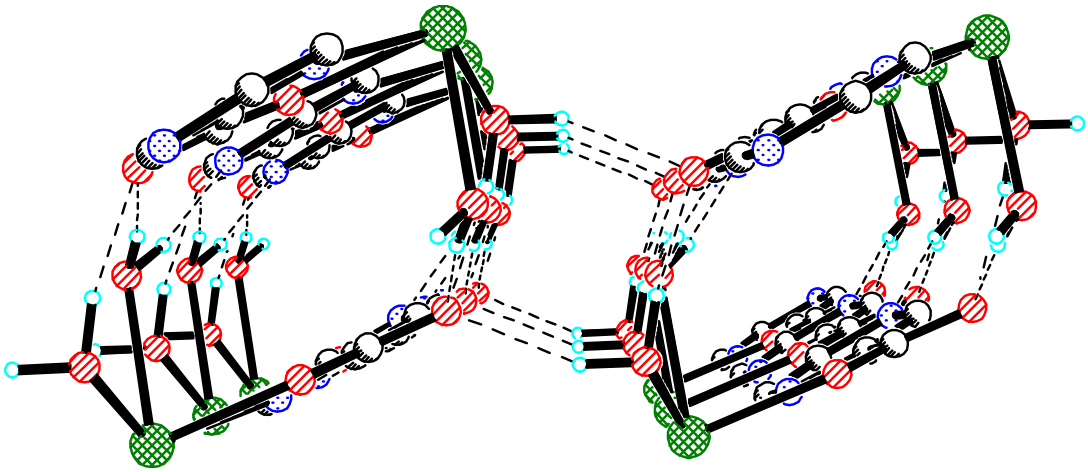

c

Fig.S3. Hydrogen bonds in the structure of **4** (Dy). Projection along axis: *x* (a); *y*, one layer is shown (b);*z* (c).

IR study of 1-9

Firstly, it should be mentioned that since compounds **1-9** are isostructural, their IR spectra are similar. However, the detailed assignment of the most characteristic bands in the spectra of **1-9** is quite difficult, since these bands strongly overlap with the bands in the IR spectra of the initial compounds.

Nevertheless, the formation of complexes **1-9** is evidenced *via* comparative analysis of the IR spectra of **1-9** and of the initial reagents, $Ln(acac)_3 \cdot 3H_2O$ and PyrCOOH, in the region of C-H stretching vibrations, i.e. 2850-3100 cm^{-1} (Fig. S4). It can be seen that the most intensive ν(C-H) bands in IR spectra of **1-9** are shifted toward lower frequencies in comparison to those in the spectrum of PyrCOOH. This can be due to the deprotonation of the PyrCOOH or to the presence of a significant amount of single C-H bonds formed by sp^3-hybridized C atoms in the $acac^-$ fragments of **1-9**, whereas almost only $C(sp^2)$-H* bonds are present in PyrCOOH and $PyrCOO^-$.[18] The latter assumtion is confirmed by almost identical location of the band near 2920 cm^{-1} in the IR spectra of **4** and $Dy(acac)_3 \cdot 3H_2O$. Since the described differences persisted while multiple registrations of IR spectra, we can conclude about their significance.

Thus, a comparative analysis of the ν(C-H) bands in IR spectra of **1-9** and similar compounds can be used as a sufficiently reliable preliminary proof of the formation of such complexes.

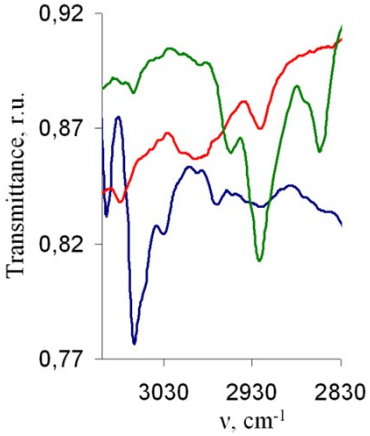

Fig. S4. IR spectra of compound **4** (green line) in comparison with IR spectra of PyrCOOH (dark blue line) and $Dy(acac)_3 \cdot 3H_2O$ (red line) in the range of 3100-2830 cm^{-1}.

As it can be seen from Fig. 2, in the IR spectra of **1-9 there is also a ν(C(sp²)-H) stretching band (≈3060 cm⁻¹), but its intensity is greatly reduced in comparison with those in the IR spectrum of PyrCOOH. The presence of very weak bands in the region of 3100-3000 cm⁻¹ in $Ln(acac)_3 \cdot 3H_2O$ is also explained by the presence of C(sp²)-H bonds in their structures with the participation of sp²-hybridized C atoms that are part of the chelating cycles.*

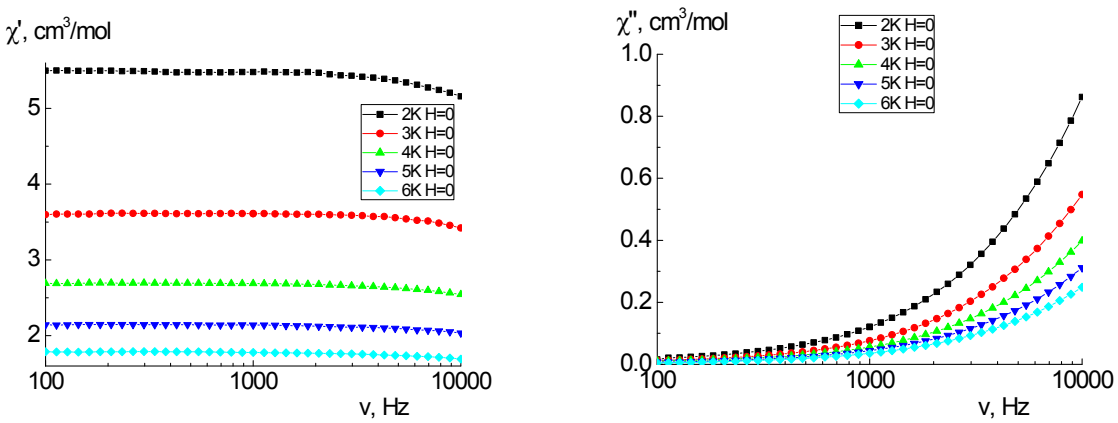

Fig. S5. Frequency dependence of the in-phase χ' (left) and out-of-phase χ″ (right) components of the *ac* susceptibility for complex **4** (Dy) in the zero *dc* field (2-6 K, step 1 K). Solid lines are visual guides.

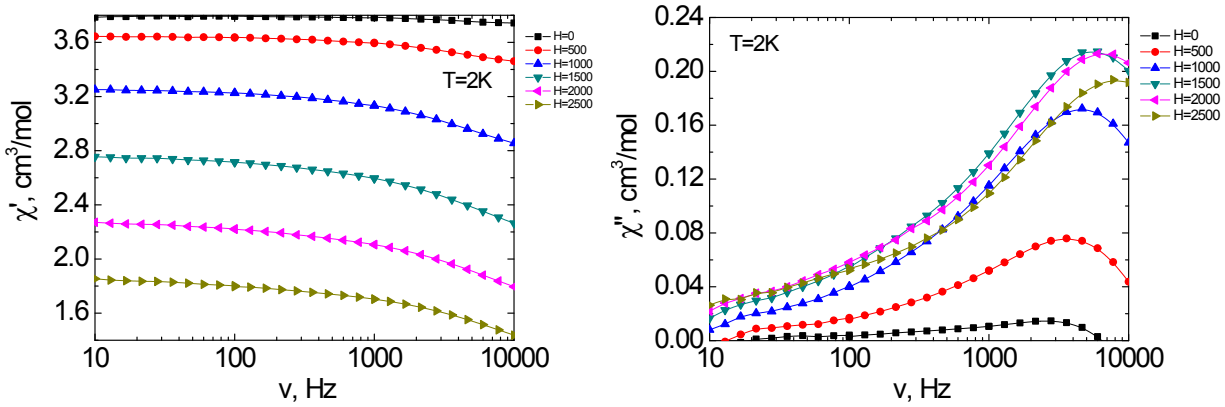

Fig. S6. Frequency dependence of the in-phase χ' (left) and out-of-phase χ″ (right) components of the *ac* susceptibility for complex **3** (Tb) in different *dc* magnetic fields (2-6 K, step 1 K). Solid lines are visual guides.

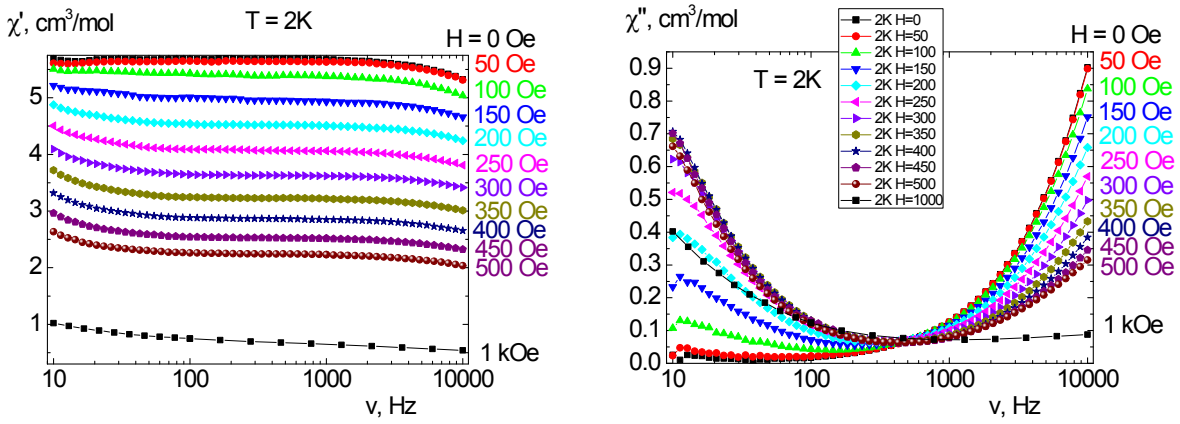

Fig. S7. Frequency dependence of χ' (left) and χ'' (right) for a polycrystalline sample of **4** (Dy) at 2 K under 0-500 Oe (Step 50 Oe) *dc* fields.

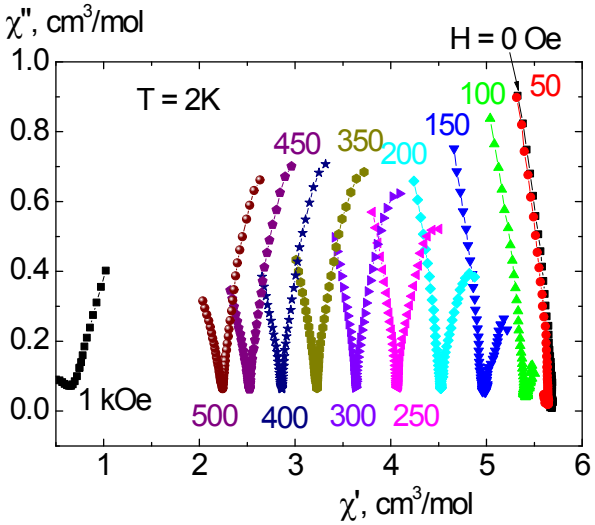

Fig. S8. Cole-Cole plots for a polycrystalline sample of **4** (Dy) at 2 K under 0-500 Oe (Step 50 Oe) *dc* field.

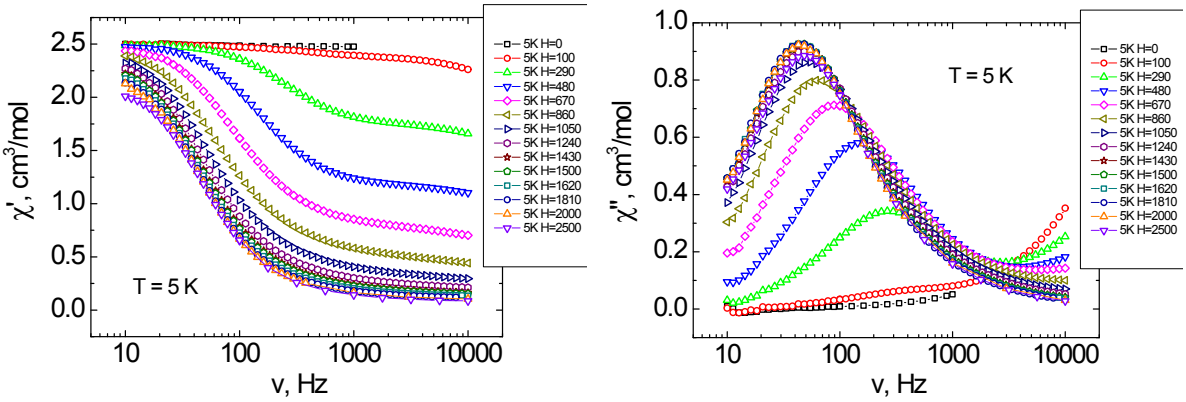

Fig. S9. Frequency dependence of χ' (left) and χ'' (right) for a polycrystalline sample of **4** (Dy) at 5 K under 0-2500 Oe *dc* fields.

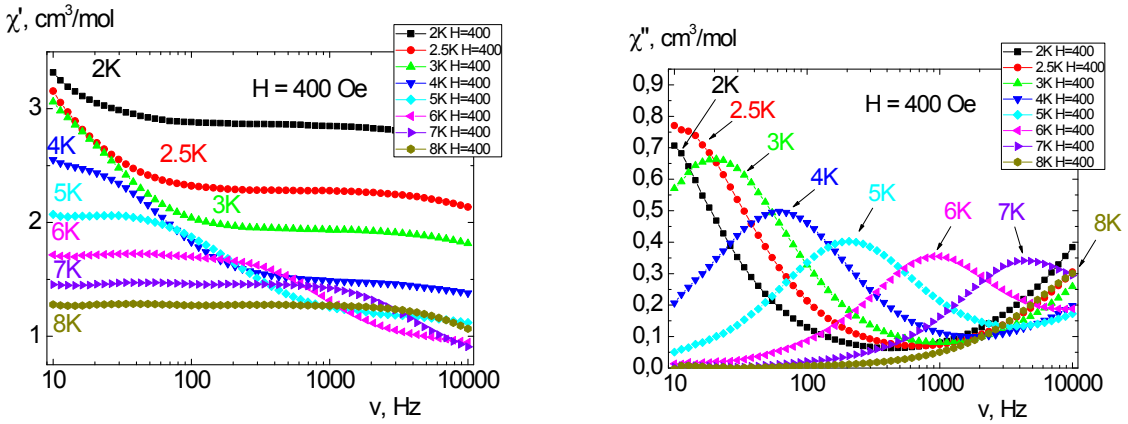

Fig. S10. Frequency dependences of the in-phase χ' (left) and out-of-phase χ″ (right) components of the *ac* susceptibility of complex **4** (Dy) in an external *dc* magnetic field of 400 Oe.

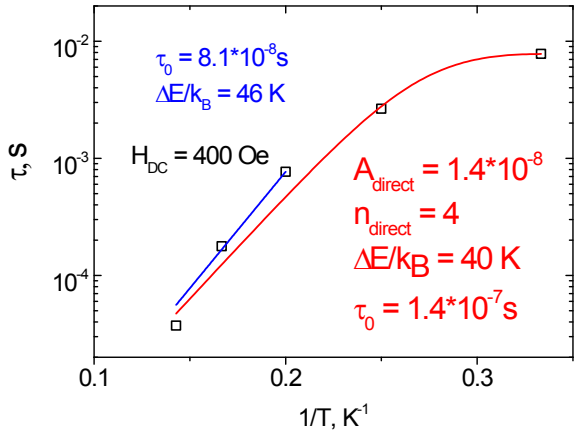

Fig. S11. Dependence of relaxation time on inverse temperature for complex **4** (Dy) (the points are based on data of frequency dependences of ac susceptibility in an external magnetic field H = 400 Oe). Solid lines are the best fit by the Arrhenius law (blue) and by the sum of direct and Orbach processes (red).

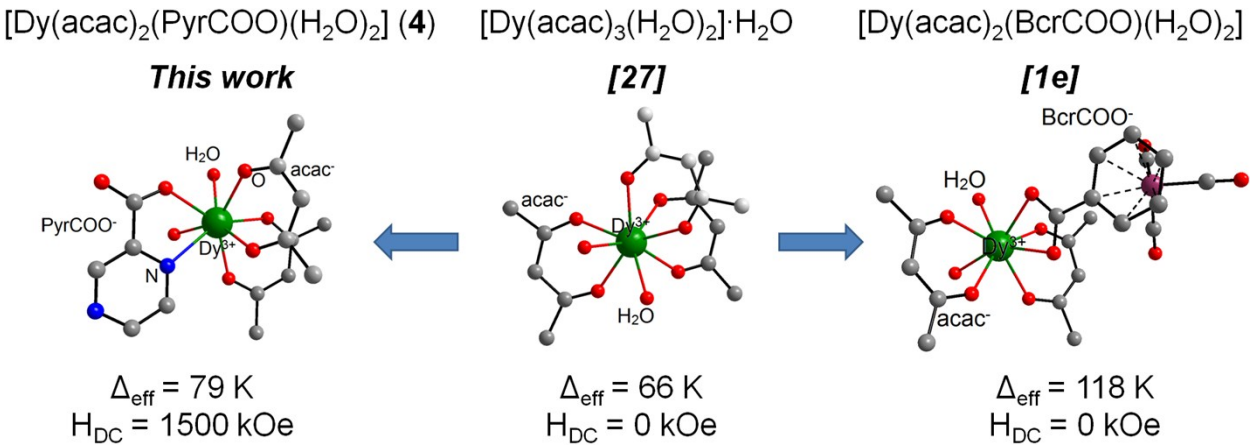

Fig. S12. Δ_{eff}/k_B values for three structurally and synthetically related complexes bearing the same $\{Dy(acac)_2(H_2O)_2\}^-$ moiety. and containing different anionic chelating ligands.

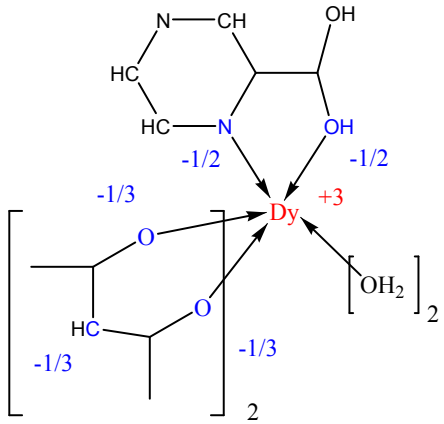

Scheme S1. Partial charges assigned to complex **4**.

Output file of MAGELLAN program assuming charges according to Scheme S1.

Site	Optimized energy (cm^{-1})	Curvature eigenvalues		Min. reversal energy (cm^{-1})
1	-0.1673E+03	0.5196E+03	0.1546E+03	0.1422E+03

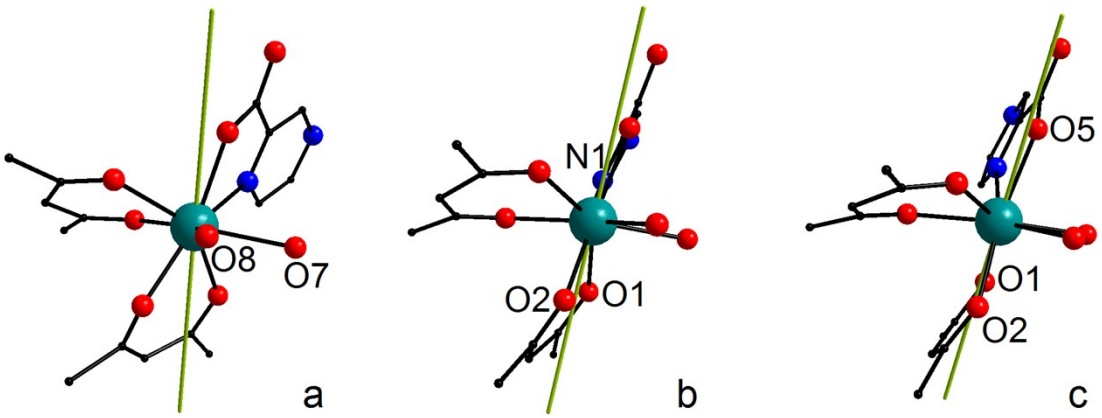

Fig. S13. Calculated magnetic anisotropy axe in **4** assuming charges according to Scheme S1.

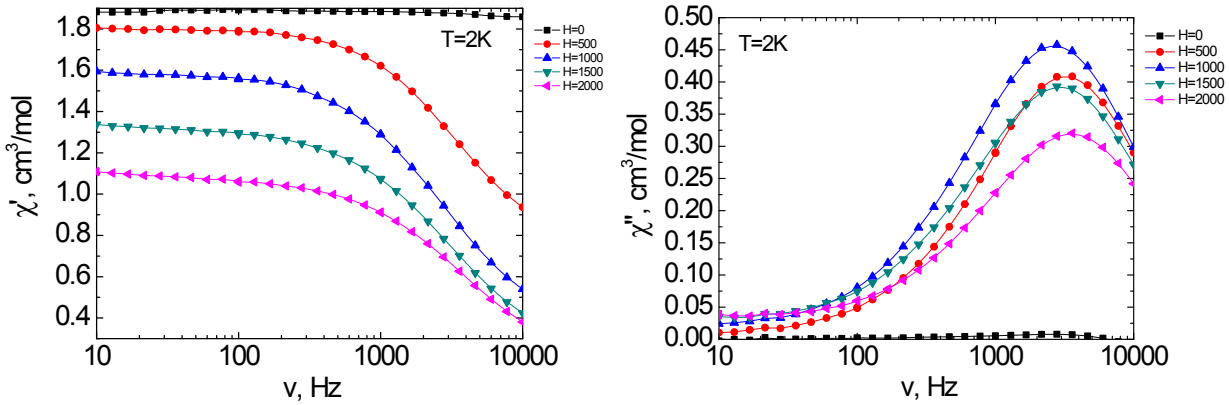

Fig. S14. Frequency dependence of χ' (left) and χ'' (right) for a polycrystalline sample of **6** (Er) at 2 K under 0- 2000 Oe (Step 500 Oe) *dc* fields.

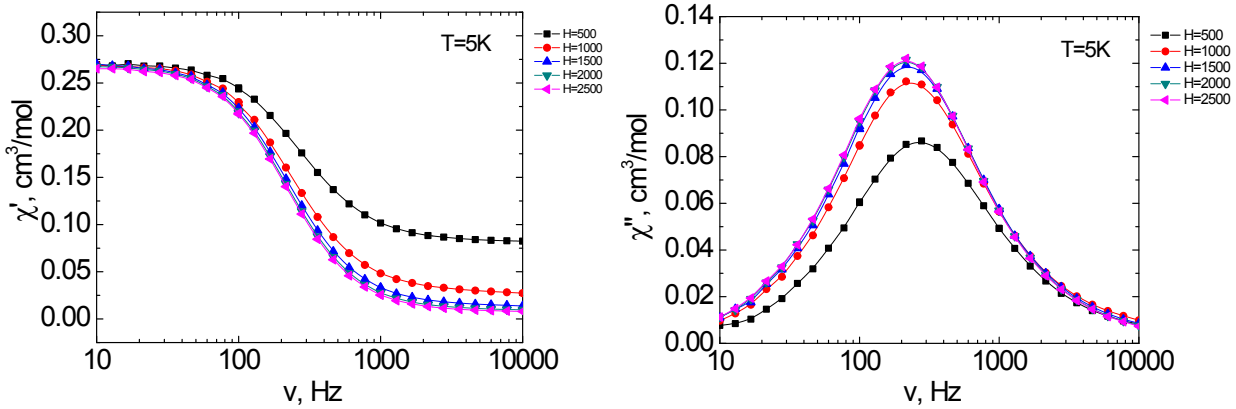

Fig. S15. Frequency dependence of χ' (left) and χ'' (right) for a polycrystalline sample of **8** (Yb) at 5 K under 0-2500 Oe (Step 500 Oe) *dc* fields.

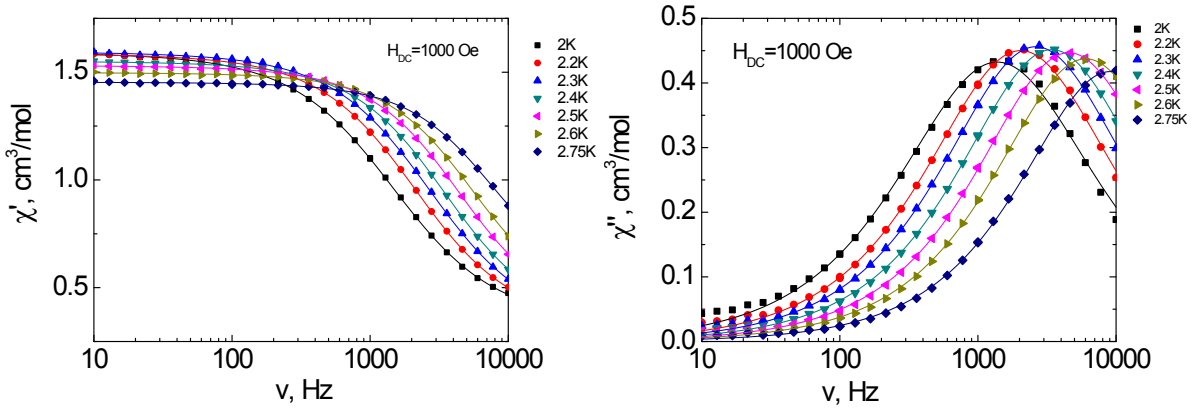

Fig. S16. Frequency dependences of the in-phase χ' (left) and out-of-phase χ″ (right) components of the *ac* susceptibility of complex **6** (Er) in an external *dc* magnetic field of 1000 Oe. Solid lines were fitted using the generalized Debye model.

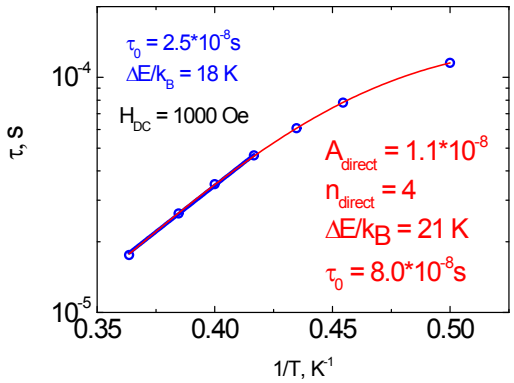

Fig. S17. Dependence of relaxation time *vs.* inverse temperature for complex **6** (Er). The points are based on data of frequency dependences of imaginary part of *ac* susceptibility in an external *dc* magnetic field of H_{dc} = 1000 Oe. Solid lines are the best fit by the Arrhenius law (blue) and by the sum of direct and Orbach processes (red).

Table S4. Structural data and SMM characteristics of mononuclear Ln carboxylate complexes.

Compound	Structure	Selected Ln-L bond lengths, Å		Δ_{eff}/k_B, K	τ_0, s	Ref.
This paper						
$[Dy(acac)_2(PyrCOO)(H_2O)_2]$	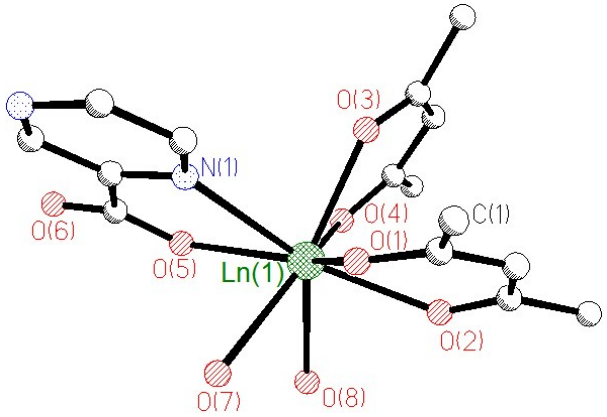	**Dy(1)-O(2)**	**2.275(4)**	H_{dc} = 1500 Oe		-
		Dy(1)-O(3)	**2.290(4)**	79	$8.5\cdot10^{-10}$	
		Dy(1)-O(1)	**2.303(4)**			
		Dy(1)-O(4)	**2.317(4)**			
		Dy(1)-O(5)	2.376(4)			
		Dy(1)-O(7)	2.435(4)			
		Dy(1)-O(8)	2.445(4)			
		Dy(1)-N(1)	2.590(4)			
$[Er(acac)_2(PyrCOO)(H_2O)_2]$		**Er(1)-O(2)**	**2.261(4)**	H_{dc} = 1000 Oe		
		Er(1)-O(3)	**2.261(5)**	18	$2.5\cdot10^{-8}$	
		Er(1)-O(1)	**2.289(4)**			
		Er(1)-O(4)	**2.296(4)**			
		Er(1)-O(5)	2.352(4)			
		Er(1)-O(7)	2.408(4)			
		Er(1)-O(8)	2.411(4)			
		Er(1)-N(1)	2.557(4)			
$[Yb(acac)_2(PyrCOO)(H_2O)_2]$		**Yb(1)-O(2)**	**2.239(3)**	H_{dc} = 2000 Oe		
		Yb(1)-O(3)	**2.255(3)**	55	$2.1\cdot10^{-8}$	
		Yb(1)-O(1)	**2.270(3)**			
		Yb(1)-O(4)	**2.279(3)**			
		Yb(1)-O(5)	2.328(3)			
		Yb(1)-O(7)	2.385(3)			
		Yb(1)-O(8)	2.399(3)			
		Yb(1)-N(1)	2.550(3)			

Compound	Structure	Selected Ln-L bond lengths, Å		Δ_{eff}/k_B, K	τ_0, s	Ref.
Literature data						
$[Tb(acac)_2(BcrCOO)(H_2O)_2]$	* 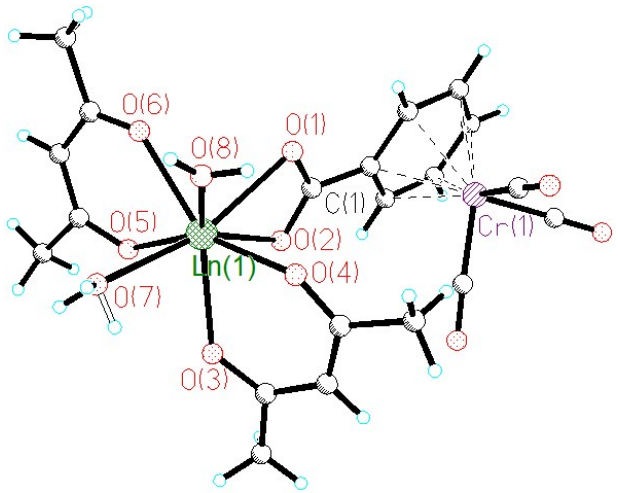	**Tb(1)-O(4)**	**2.3015(18)**	H_{dc} = 2000 Oe		[1e]
		Tb(1)-O(6)	**2.3423(18)**	5	$4 \cdot 10^{-6}$	
		Tb(1)-O(5)	**2.3665(18)**			
		Tb(1)-O(3)	**2.3674(17)**			
		Tb(1)-O(8)	2.4102(19)			
		Tb(1)-O(2)	2.4279(17)			
		Tb(1)-O(1)	2.4302(18)	H_{dc} = 0 Oe		
		Tb(1)-O(7)	2.430(2)			
$[Dy(acac)_2(BcrCOO)(H_2O)_2]$		**Dy(1)-O(4)**	**2.2838(18)**	100 (*LF*) 118 (*HF*)	$5.6 \cdot 10^{-7}$ (*LF*) $4.5 \cdot 10^{-8}$ (*HF*)	
		Dy(1)-O(6)	**2.3232(18)**			
		Dy(1)-O(5)	**2.3516(17)**			
		Dy(1)-O(3)	**2.3557(17)**			
		Dy(1)-O(8)	2.4019(18)	H_{dc} = 2000 Oe		
		Dy(1)-O(1)	2.4176(18)			
		Dy(1)-O(7)	2.4184(19)	128 (*LF*) 143 (*HF*)	$3.0 \cdot 10^{-8}$ (*LF*) $7.1 \cdot 10^{-8}$ (*HF*)	
		Dy(1)-O(2)	2.4191(18)			

$acac^-$ = acetylacetonate (pentane-2,4-dionate) anion; $PyrCOO^-$ = pyrazine-2-carboxylate anion,
$BcrCOO^-$ = anion of (κ^6-benzoic acid)tricarbonylchromium.
* This figure is reproduced from [1e] with changes in appearance.

Table S5. Δ_{eff}/k_B and τ_0, values for known Ln^{3+} carboxylate complexes exhibiting SMM properties.

Compound / *NUCLEARITY*	**Δ_{eff}/k_B, K**	**τ_0, s**	**Ref.**
This paper			
$[Dy(acac)_2(PyrCOO)(H_2O)_2]$ / *MONONUCLEAR* acac$^-$ = acetylacetonate (pentane-2,4-dionate) anion; PyrCOO$^-$ = pyrazine-2-carboxylate anion	H_{dc} = 1500 Oe		-
	77 (d.+O.)	$8.4\cdot10^{-10}$ (d.+O.)	
$[Er(acac)_2(PyrCOO)(H_2O)_2]$ / *MONONUCLEAR*	H_{dc} = 1000 Oe		
	21 (d.+O.)	$8.0\cdot10^{-9}$ (d.+O.)	
$[Yb(acac)_2(PyrCOO)(H_2O)_2]$ *MONONUCLEAR*	H_{dc} = 2000 Oe		
	54 (d.+O.+R.)	$7.4\cdot10^{-8}$ (d.+O.+R.)	
Literature data			
$[Tb(acac)_2(BcrCOO)(H_2O)_2]$ / *MONONUCLEAR* acac$^-$ = acetylacetonate (pentane-2,4-dionate) anion; BcrCOO$^-$ = anion of (κ^6-benzoic acid)tricarbonylchromium	H_{dc} = 2000 Oe		[1e]
	5	$4\cdot10^{-6}$	
$[Dy(acac)_2(BcrCOO)(H_2O)_2]$ / *MONONUCLEAR*	H_{dc} = 0 Oe		[1e]
	100 (*LF*) 118 (*HF*)	$5.6\cdot10^{-7}$ (*LF*) $4.5\cdot10^{-8}$ (*HF*)	
	H_{dc} = 2000 Oe		
	128 (*LF*) 143 (*HF*)	$3.0\cdot10^{-8}$ (*LF*) $7.1\cdot10^{-8}$ (*HF*)	
$[Dy_2(3\text{-}Htzba)_2(3\text{-}tzba)_2(H_2O)_8]\cdot4H_2O$ / *BINUCLEAR* 3-Htzba, 3-tzba = mono- and dianion of 3-(1H-tetrazol-5-yl) benzoic acid, respectively	H_{dc} = 0 Oe		[12a]
	53.7	$1\cdot10^{-2}$	
	H_{dc} = 2000 Oe		
	54.8	$1.1\cdot10^{-9}$	
$[Dy_2(anthc)_6(bpy)_2]$ / *BINUCLEAR* anthc$^-$ = 9-anthracene-carboxylate; bpy = 2,2`-bipyridyl	H_{dc} = 0 Oe		[12i]
	51.2	$3.2\cdot10^{-8}$	

Compound / *NUCLEARITY*	Δ_{eff}/k_B, **K**	τ_0, **s**	**Ref.**
$[Dy_2(anthc)_6(phen)_2]$ / *BINUCLEAR* phen = 1,10-phenantroline	H_{dc} = 0 Oe		
	49.4	$4.6\cdot10^{-9}$	
$[Dy_2(anthc)_6(dmphen)_2]$ / *BINUCLEAR* dmphen = 4,7-dimethyl-1,10-phenantroline	H_{dc} = 0 Oe		
	31.6	$3.4\cdot10^{-8}$	
$[Dy_2(CymCOO)_4(NO_3)_2(DMSO)_4]$ / *BINUCLEAR* *CymCOO$^-$ – anion of* of (κ^5-cyclopentadienecarboxylic acid) tricarbonylmanganese	H_{dc} = 0 Oe		[12b]
	53	$3.2\cdot10^{-9}$	
$[Dy_3(HSA)_5(SA)_2(phen)_3]$ / *TRINUCLEAR* HSA, SA = mono- and dianion of salicylic (2-hydroxybenzoic) acid, respectively	H_{dc} = 0 Oe		[6d]
	65	$1.5\cdot10^{-5}$	
$[Dy_4(L)_4(Piv)_4]\cdot4H_2O\cdot6CH_3OH$ / *TETRANUCLEAR* H_2L = (E)-2-((6-(hydrixymethyl)pyridine-2-yl)methyleneamino)phenol; PivH – pivalic (trimethylacetic) acid	H_{dc} = 0 Oe		[12g]
	23.8 (-*QT*) 43.4 (+*QT*)	$1.3\cdot10^{-5}$ (-*QT*) $8\cdot10^{-7}$ (+*QT*)	
	H_{dc} = 1000 Oe		
	37 (*FR*/*HF*) 73 (*SR*/*LF*)	$2.7\cdot10^{-6}$ (*FR*/*HF*) $4.4\cdot10^{-8}$ (*SR*/*LF*)	
$[Dy_6(spch)_6(O_3PC_{10}H_7)_2(PyrCOO)_2(MeOH)(H_2O)]\cdot8.5H_2O$ / *HEXANUCLEAR* H_2spch = (E)-N`-(2-hydroxybenzylidene)pyrazine-2-carbohydrazide; PyrCOO$^-$ = pyrazine-2-carboxylate anion	H_{dc} = 0 Oe		[12d]
	20.3 (*HTR*) 4.7 (*LTR*)	$2.6\cdot10^{-6}$ (*HTR*) $9.1\cdot10^{-5}$ (*LTR*)	
$[Dy_7(eddc)_6(spch)_2(O_3PC_{10}H_7)_4(OAc)_5(MeOH)_4]\cdot 4MeOH$ / *HEPTANUCLEAR* H_2eddc = (E,E)-N`,N``-(ethane-1,2-diylidene)bis(pyrazine-2-carbohydrazide)	H_{dc} = 0 Oe		
	48.7 (*HTR*) 45.1 (*LTR*)	$2.7\cdot10^{-8}$ (*HTR*) $4.4\cdot10^{-7}$ (*LTR*)	
$[Dy(\mu^3\text{-}OH)(na)(PyrCOO)]_n$ / *1D-POLYMERIC* na = 1-naphtolate anion	H_{dc} = 3000 Oe		[12e]
	39.6	$1.52\cdot10^{-8}$	
$[Dy(acac)_2(BcrCOO)(H_2O)]_n$ / *1D-POLYMERIC*	H_{dc} = 2000 Oe		[1e]

Compound / *NUCLEARITY*	Δ_{eff}/k_B, **K**	τ_0, **s**	**Ref.**
	38	$6\cdot10^{-7}$	
$[Dy(acac)_2(CymCOO)(H_2O)]_n$ / *1D-POLYMERIC*	H_{dc} = 2000 Oe		[12b]
$[Dy(acac)_2(CymCOO)(H_2O)]_n$ / *1D-POLYMERIC*	42	$4.3\cdot10^{-7}$	
$[Dy_2(CymCOO)_6(H_2O)_4]_n$ / *1D-POLYMERIC*	H_{dc} = 0 Oe		
	4.1	$4.3\cdot10^{-6}$	
$\{[Dy_2(dae)_3(DMSO)_3(MeOH)]\cdot10MeOH\}_n$ / *2D-POLYMERIC*	H_{dc} = 1500 Oe		[12c]
	14.2	$1.90\cdot10^{-8}$	
$\{[Ho_2(dae)_3(DMSO)_3(MeOH)]\cdot10MeOH\}_n$ / *2D-POLYMERIC*	H_{dc} = 1500 Oe		
	14.4	$7.49\cdot10^{-8}$	
$[Er(acac)_2(BcrCOO)(H_2O)]_n$ / *1D-POLYMERIC*	H_{dc} = 2000 Oe		[1e]
	57 (*LF*) 14 (*HF*)	$1.2\cdot10^{-10}$ (*LF*) $7.3\cdot10^{-7}$ (*HF*)	
$[Yb(\mu^3\text{-}OH)(na)(PyrCOO)]_n$ / *1D-POLYMERIC*	H_{dc} = 3000 Oe		[12e]
	14.1	$2.13\cdot10^{-7}$	
$\{[Yb(L)(H_2O)_3(DMF)]\cdot(HL)\cdot(H_2O)\}_n$ / *1D-POLYMERIC* L = dianion of 4,5-bis(carboxylic)-4`,5`-methyldithiotetrathiafulvene	H_{dc} = 1000 Oe		[12f]
	28 3.2	$3.3\cdot10^{-7}$ $2.0\cdot10^{-4}$	
$[Yb(acac)_2(BcrCOO)(H_2O)]_n$ / *1D-POLYMERIC*	H_{dc} = 2000 Oe		[1e]
	36	$1.5\cdot10^{-7}$	

(d.+O.) – fitting with the sum of direct (d.) and Orbach (O.) relaxation mechanisms.

(d.+O.+R.) – fitting with the sum of direct (d.), Orbach (O.) and Raman (R.) relaxation mechanisms;

LF – low-frequency mode;

HF – high-frequency mode;

-*QT* – without quantum tunneling contribution;

+*QT* – with quantum tunneling contribution;

FR – fast relaxation; *SR* – slow relaxation;

HTR – high-temperature relaxation;

LTR – low-temperature relaxation.